Supplementary Information for

Mineral Formation in the Primary Polyps of Pocilloporoid Corals

Maayan Neder[a,b], Pierre Philippe Laissue[c], Anat Akiva[d], Derya Akkaynak[b,e], Marie Albéric[f], Oliver Späker[f], Yael Politi[f], Iddo Pinkas[g*] and Tali Mass[a*]

[a] Department of Marine Biology, The Leon H. Charney School of Marine Sciences, University of Haifa, Mt. Carmel, Haifa 3498838, Israel
[b] The Interuniversity Institute of Marine Sciences, Eilat 88103, Israel
[c] School of Biological Sciences, Wivenhoe Park, University of Essex, Colchester CO4 3SQ, UK.
[d] Laboratory of Materials and Interface Chemistry and Center for Multiscale Electron Microscopy, Department of Chemical Engineering and Chemistry and Institute for Complex Molecular Systems, Eindhoven University of Technology, 5600 MB Eindhoven, The Netherlands
[e] Department of Marine Technologies, The Leon H. Charney School of Marine Sciences, University of Haifa, Mt. Carmel, Haifa 3498838, Israel
[f] Max-Planck Institute of Colloids and Interfaces Potsdam- Golm 14476, Germany
[g] Department of Chemical Research Support, Weizmann Institute of Science, Rehovot 76100, Israel

* Correspondence to: tmass@univ.haifa.ac.il, iddo.pinkas@weizmann.ac.il

Supplementary data

Movie 1- 24h time lapse series of the periphery dumbbells merging to form the septum in one day settled *S. pistillata* primary polyp

Movie 2- 24h time lapse series of the dumbbells merging to form the basal plate in three days settled *S. pistillata* primary polyp (see also Fig. 2)

Movie 3- DIC 12h time lapse series of one day settled *S. pistillata* primary polyp after antibiotic treatment (see materials and methods, Fig S3)

Table 1- bacterial 16S sequences and annotation from *S. pistillata* primary polyps

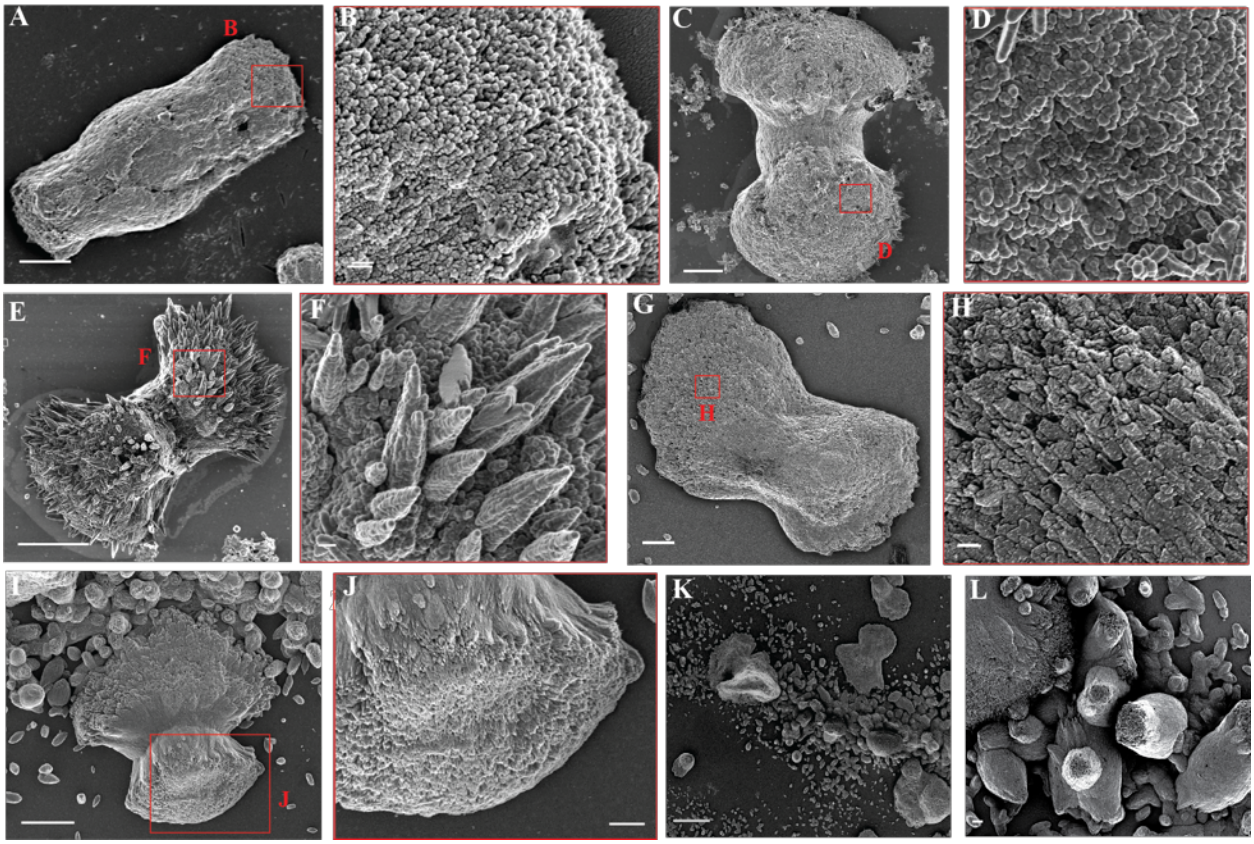

Figure 1- SEM images of several examples of *S. pistillata* (A-F) and *P. acuta* (G-L) rods and dumbbells and their ultra-structure. (A, C, G) dumbbells at early maturation states. (B, D, H) higher magnifications of the regions depicted in red boxes in A, C, and G showing that the pristine dumbbells are characterized by nano-particle granules. (E, I) developing dumbbells. (F, J) Higher magnifications of the regions depicted in red boxes in (E, I) showing that needle shaped fibers are growing on top of the dumbbells. (K) A forming septum in *P. acuta* is composed of rod-shaped building blocks, as well as dumbbell structures making up the septum wall. (L) Joined dumbbell and rod shaped structures forming the base of the septum. **Scale bar**; **A, G,** - 3 µm; **B, D, F, H, J**- 200nm; **C, E, I-** 5 µm; **J**- 2 µm ; **K**- 20 µm; **L**- 1 µm

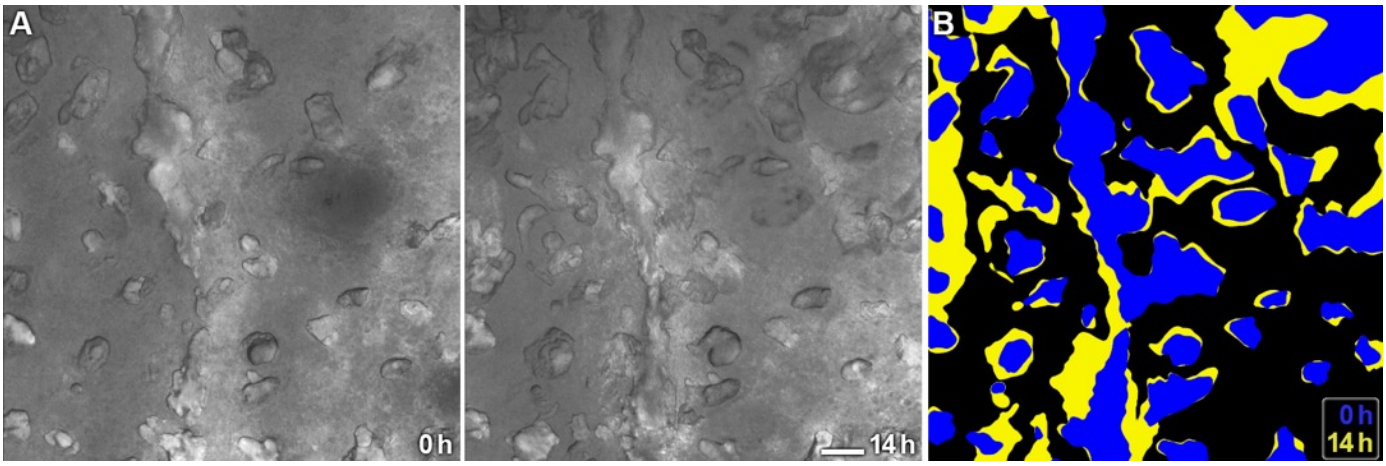

Figure 2- *S. pistillata* DIC images of *in vivo* confocal microscopy of the septa and basal plate. Time points of a 14 h time lapse series of a developing septum and the peripheral dumbbells forming the basal plate in a three day settled *S. pistillata* primary polyp (A) The first and the last time points (14 hours after the first image) (B) Overlay of false-color images of the first time point (blue) and the last time point (yellow) showing the growth pattern**. Scale bar-** 10 µm

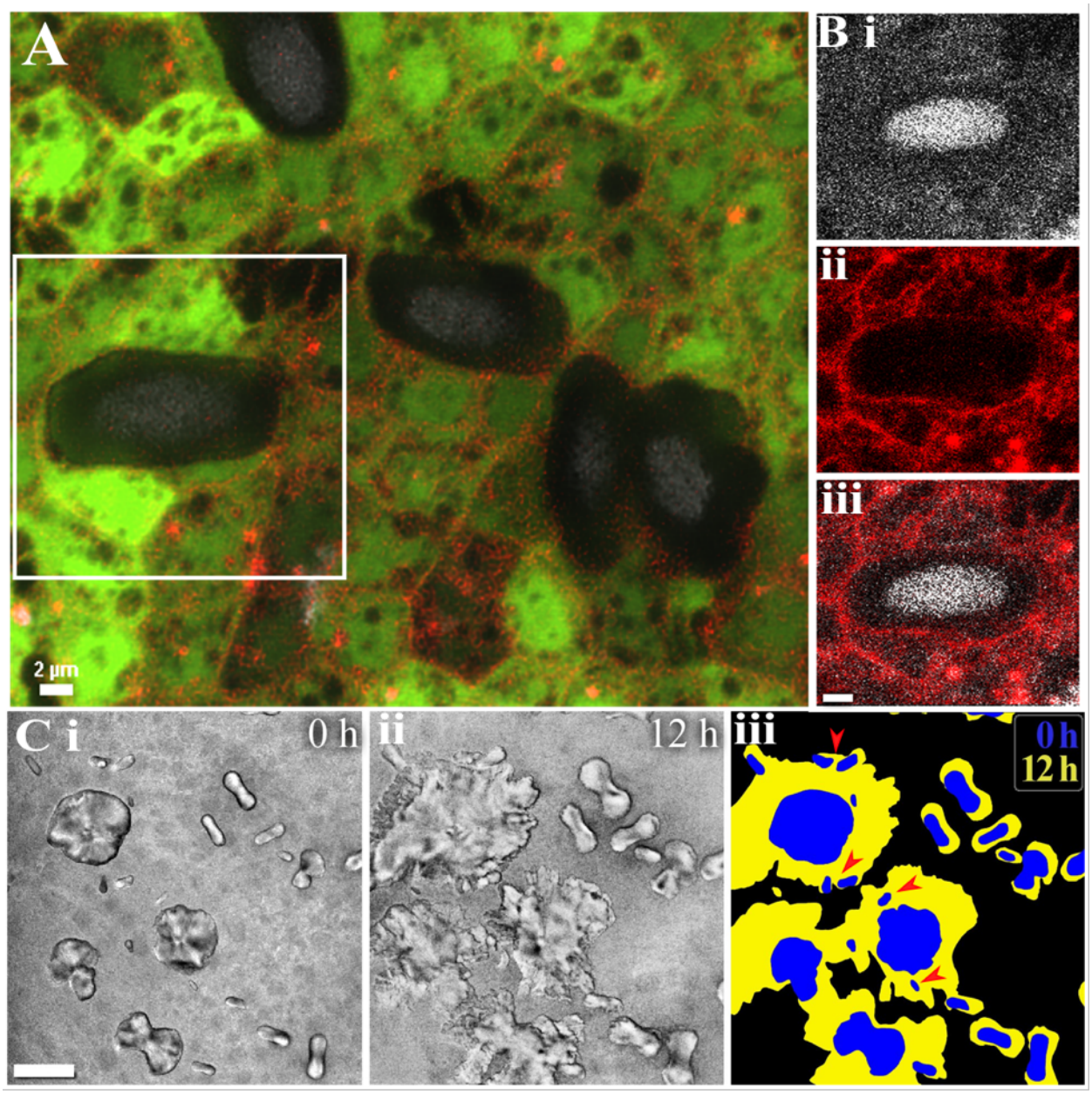

Figure 3- Bacterial assays of *S. pistillata* primary polyps, using in In vivo microscopy techniques

(A-B) *in vivo* fluorescence confocal laser scanning microscopy. Native GFP autofluorescence is displayed in green, calcein Blue fluorescence displayed in white, and FM 4-64 membrane fluorescence marker display in red. The membrane stain defines individual cell borders, intracellular compartments and the absence of bacteria around the forming dumbbell structures. (B) Higher magnification of the region depicted in the white box in (A). B i) Calcein Blue staining. ii) FM 4-64 membrane marker staining. iii) Overlay of i-ii showing seperation of the tissue and the mineral (C) DIC 12 h time-series of *S. pistillata* primary polyp after antibiotic treatment (see

methods, Supplementary movie 3). (Ci) The first time point (Cii) 12 hours after the first image (Ciii) Overlay of false-color images of (Ci, blue) and (Cii, yellow). Red arrows- pristine dumbbells. Scale bars: **A-B** 2µm; **C** 10 µm

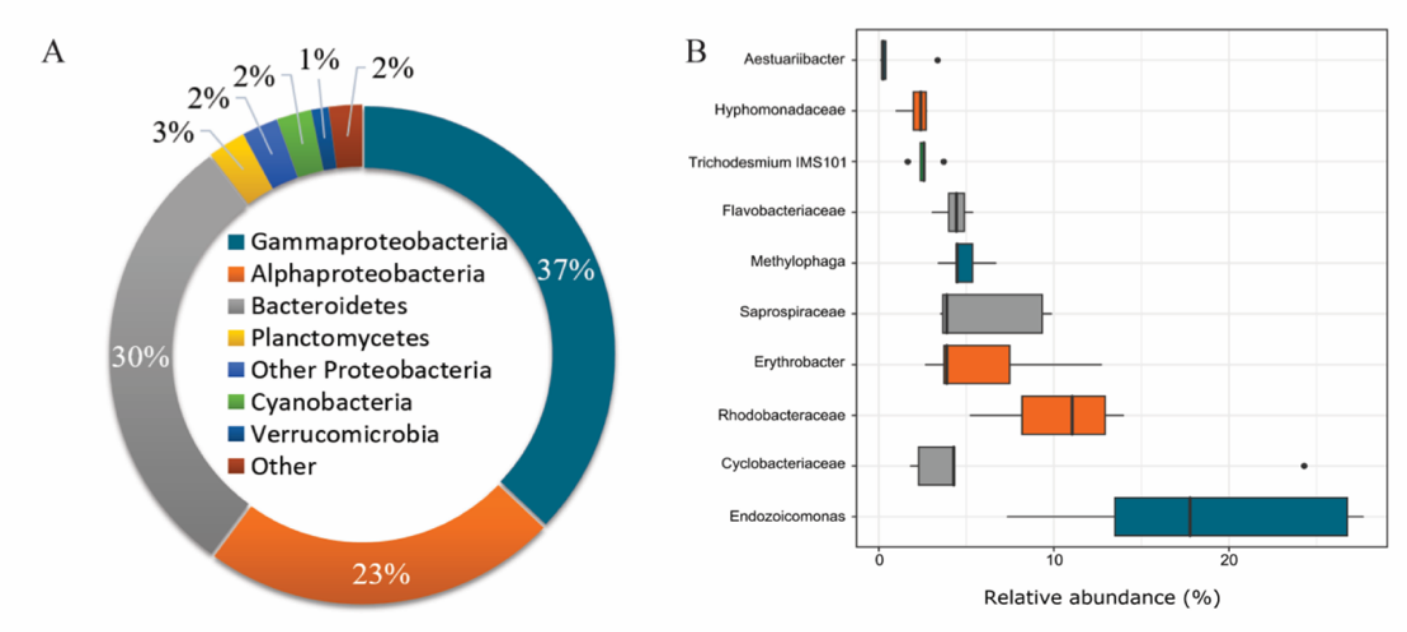

Figure 4- Composition of *S. pistillata* active bacterial community and growth pattern in bacteria free medium. (A) Relative abundance of phyla and dominant classes. (B) Contribution of the most dominant genera and families in the RNA samples of *S. pistillata*.

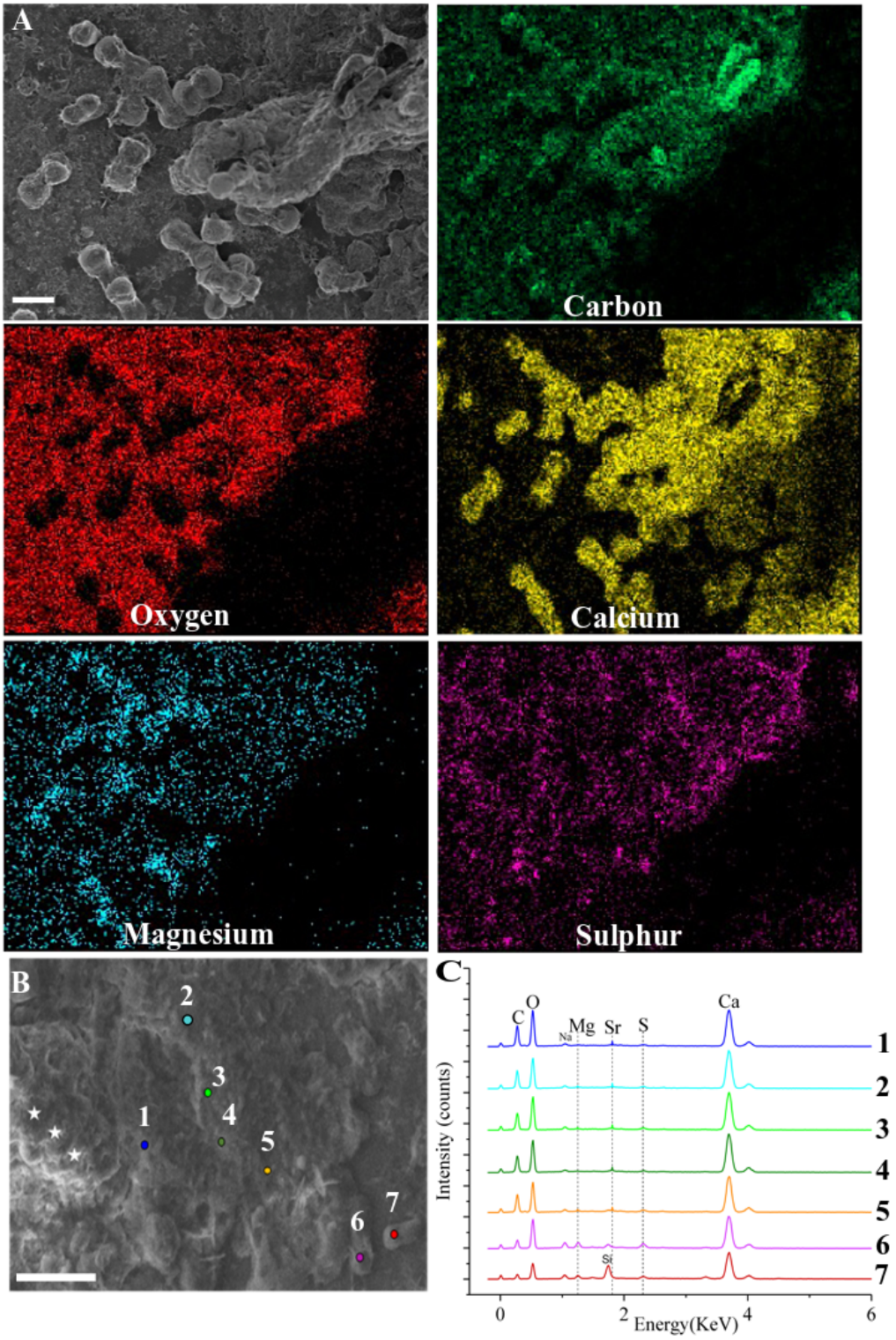

Figure 5- elemental distribution in different mineral structures in the primary polyp. Energy Dispersive X-Ray Spectroscopy (EDS) (A) map of *S. Pistillata* developed septum next to the pristine dumbbells. Each panel contains an SEM image of the areas sampled by the EDS, and the

elemental distribution maps for each of the detected ions. Carbon, oxygen, calcium, magnesium and Sulphur are observed. The pristine dumbbells are rich in magnesium, and in the developed septum, there is high concentration of sulphur, which may point to the surrounding biological matrix. (B) Basal plate closure next to the septum (white stars) and dumbbells in the periphery (points 6-7). (C) EDS spectra of points of interest in (B). The colors and the numbers of the spectra correspond to the positions numbered in (B). The pristine dumbbells contain magnesium, while the basal plate closure and the septa contains sulphur, strontium or both. **Scale bars**: A-20µm, B-25µm

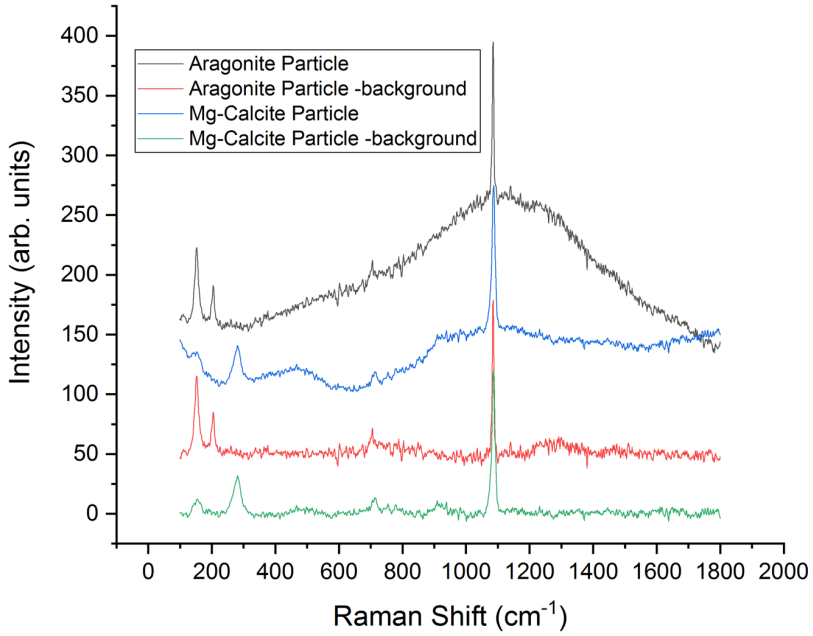

Figure 6- Raman spectra of Mg- calcite and aragonite measured in *S. pistillata* primary polyps. Black line- aragonite raw spectrum, red line- aragonite after background subjection, blue line - Mg-calcite raw spectrum and green line- Mg-calcite after background subjection.

Table S2 - Raman main peak assignments

Calcite (Ref 51)			**Mg-Calcite (this work)**			**Dolomite (Ref 54)**			**Magnesite (Ref 54)**		
Raman Shift (cm^{-1})	**Symmetry**	**#**	**Raman Shift (cm^{-1})**	**Symmetry**	**#**	**Raman Shift (cm^{-1})**	**Symmetry**	**#**	**Raman Shift (cm^{-1})**	**Symmetry**	**#**
155.5	E_g	2	157.5	E_g		177.1	E_g		213.6	E_g	
281.2	E_g	3	283.8	E_g		301.1	E_g		331	E_g	
712.4	E_g	4	715	E_g		723.9	E_g		738.1	E_g	
1086.2	A_{1g}	1	1089	A_{1g}		1098.1	A_{1g}		1094.9	A_{1g}	
1435.8	E_g	5				1442.5	E_g		1445.8	E_g	

Table 3- Raman main peak differences of the spectra from the cross section presented in Fig. 4A

Aragonite Raman Shift (cm^{-1})	Aragonite Linewidth (cm^{-1})	Mg-calcite Raman Shift (cm^{-1})	Mg-calcite linewidth (cm^{-1})
152.4	11.4	157.5	13.7
205.1	9.9	283.8	20.1
702.6	3.7	715.0	15.4
705.6	4.4		
1085.6	4.3	1089.0	10.7

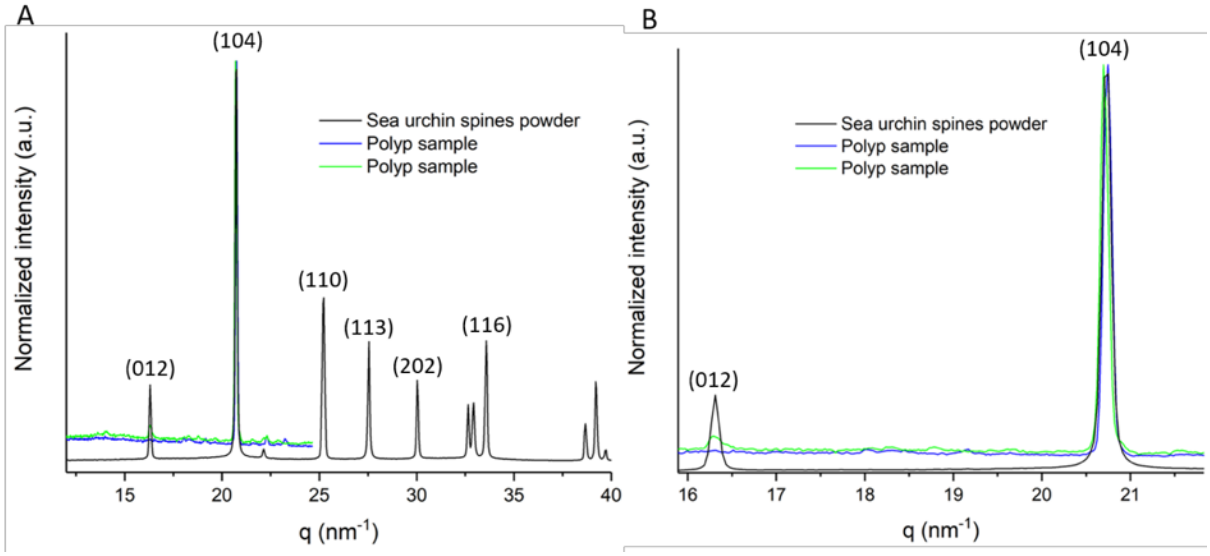

Figure 7- X-ray diffraction profiles obtained at BESSY II synchrotron at the MuSpot beamline of *S. pistillata* primary polyps (in blue and green) and reference powdered sea urchin spines (in black) for a q range of (A) 15 to 40 nm^{-1} and (B) 16 to 23 nm^{-1}. The powdered sea urchin spines sample is the one used in[1] where a Mg concentration of 3 mol% was measured, it shows a typical x-ray profile of bio-calcite with all the main reflections, in particular the (012) and (104) reflections also observed in the x-ray diffraction profiles of the primary polyps. The peak positions and their shift compared to geological or synthetic calcite may be related to the amount of Mg incorporate in the calcite crystals as the incorporation of Mg induces lattice distortion in particular a reduction of the *a* and *c* unit-cell parameters (Paquette et al. 1990). The (012) and (104) reflection in sea urchin spines and the primary polyps show similar peak positions, 16.3 and 20.7 nm^{-1}

respectively, therefore, the polyp samples may be composed of Mg-calcite having similar Mg content than in sea urchin spines, i.e. about 3 mol%.

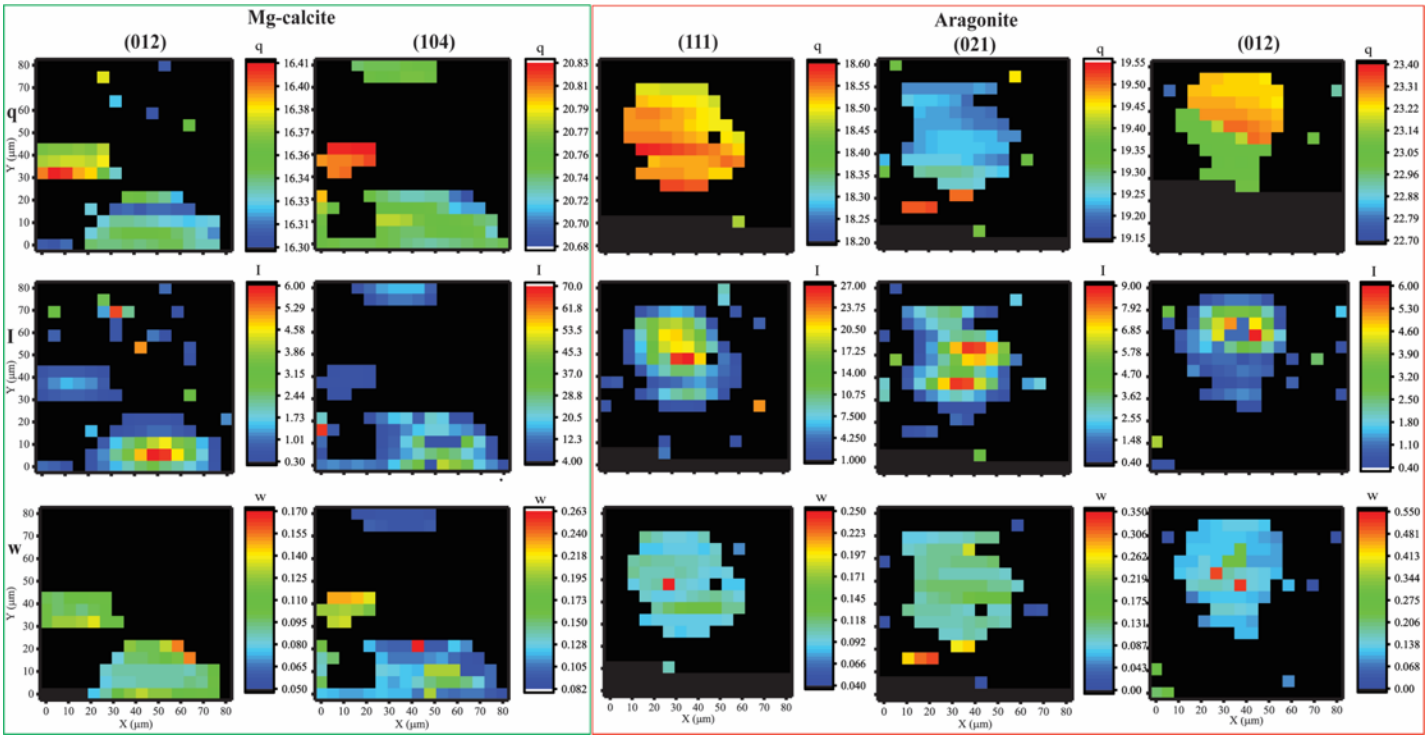

Figure 8- Scanning X-ray diffraction (XRD) 2D maps of *S. pistillata* primary polyp one day settled (the same measurement region shown in figure 5). Top row maps- peak position (q), middle row maps- peak intensity (I) and bottom row maps- peak width (w) for each reflection characterizing Mg-calcite (012 and 104) and aragonite (111, 021 and 012).

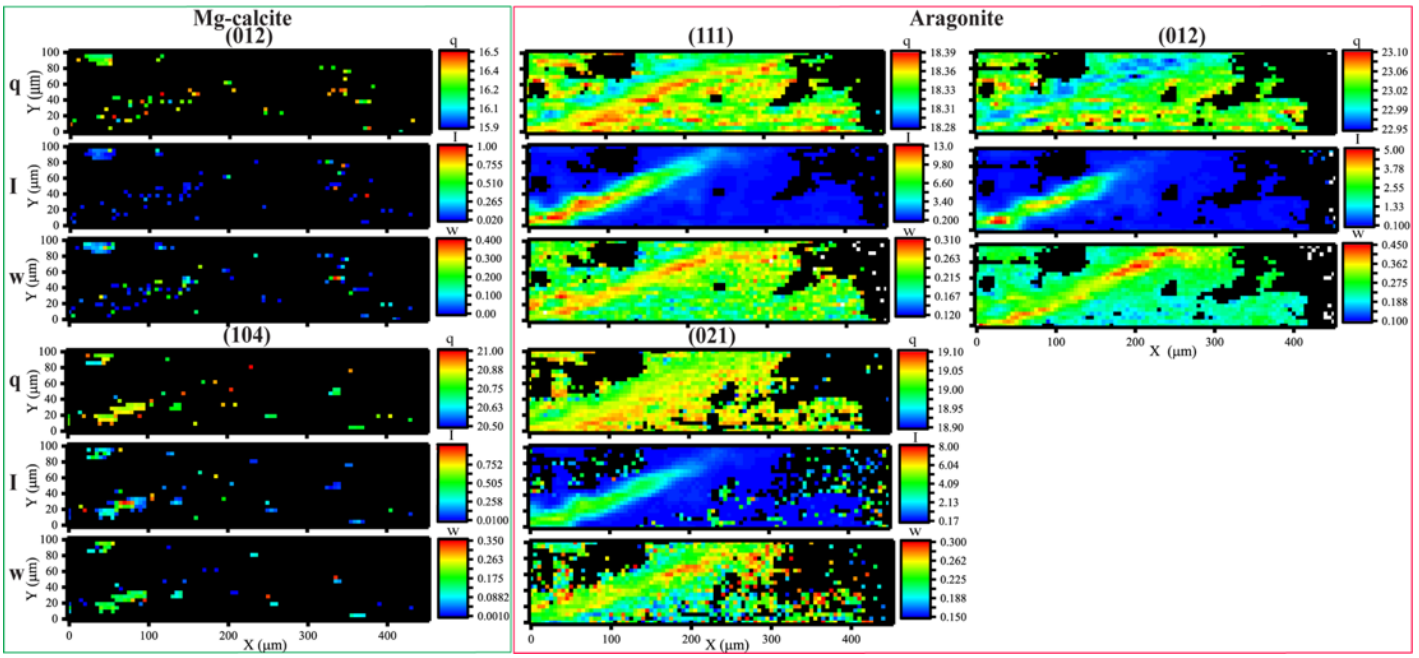

Figure 9- of X-ray diffraction (XRD) 2D maps of *S. pistillata* primary polyp two days settled- (the same measurement region shown in figure 6). Upper row of maps- peak position (q), middle row of maps– peak intensity (I), and bottom row of maps- peak width (w) of each reflection characterizing Mg-calcite (012 and 104) and aragonite (111, 021 and 012).

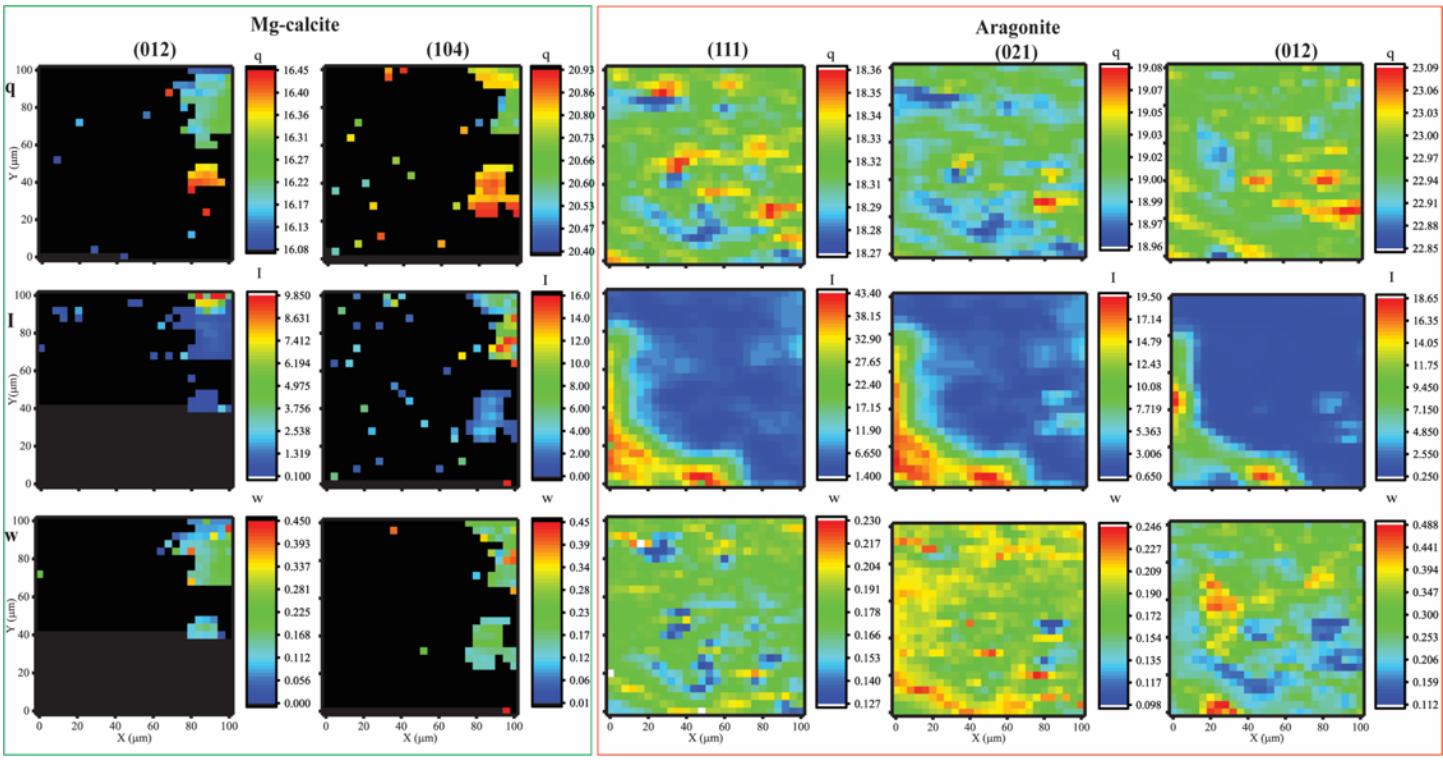

Figure 10- X-ray diffraction (XRD) 2D maps of *S. pistillata* primary polyp four days settled- Upper row of maps- peak position (q), middle row of maps– peak intensity (I), and bottom row of maps- peak width (w) of each reflection characterizing Mg-calcite (012 and 104) and aragonite (111, 021 and 012).

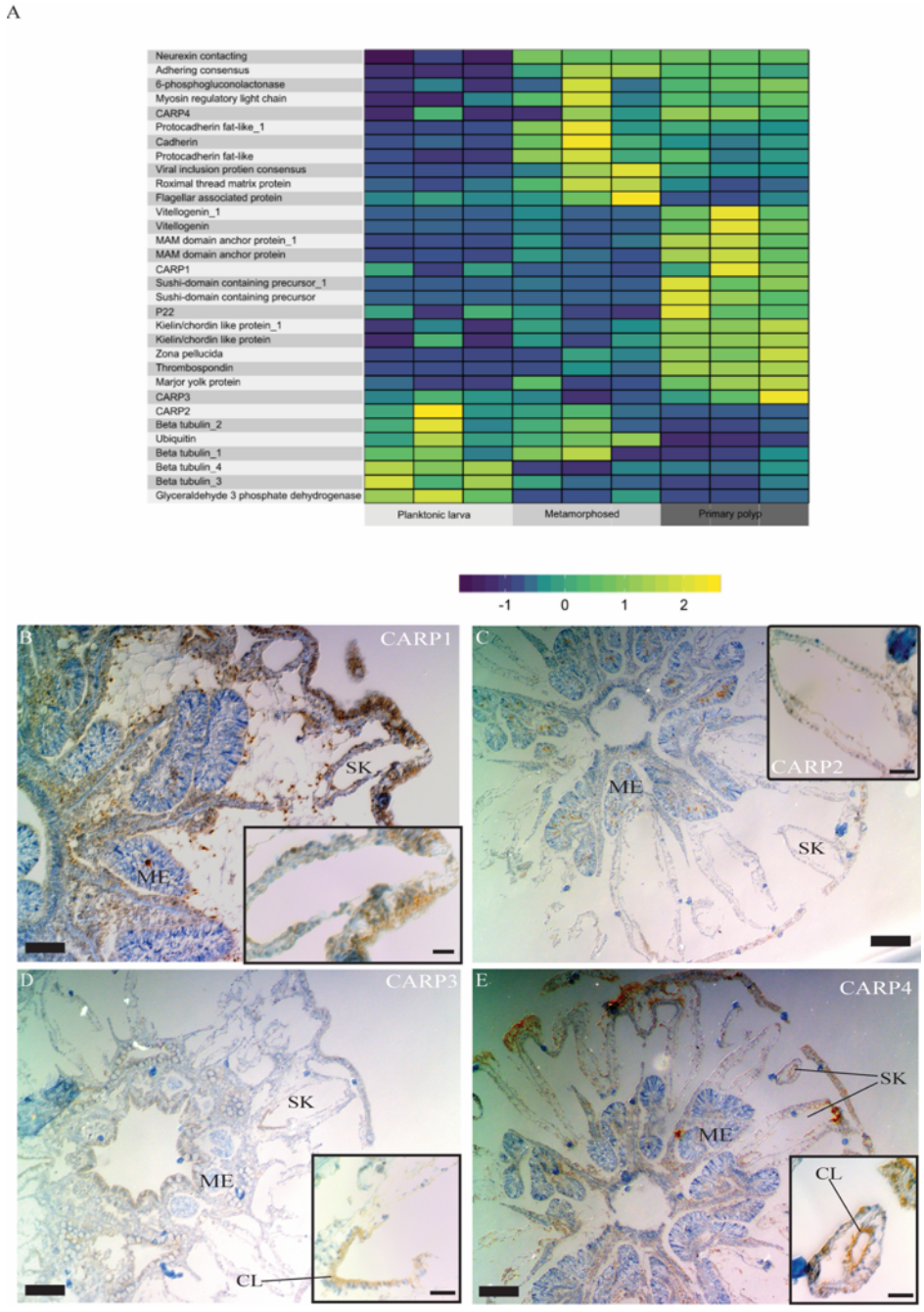

Figure 11- Expression pattern of *S. pistillata* primary polyps biomineralization tool-kit genes- (A) gene expression of biomineralization tool-kit genes which were previously described by[2], at

the three developmental stages. (B-E) Immunohistochemistry of four CARPs (1–4) in the primary polyps reveals labeling at distinct intracellular locations for each protein (brown), counterstained with hematoxylin (blue) to show nuclei. SK, skeleton side, ME- mesentery; CL- calicoblastic layer. **Scale bar**; external B-E 20 µm; Insets B-E 5 µm.

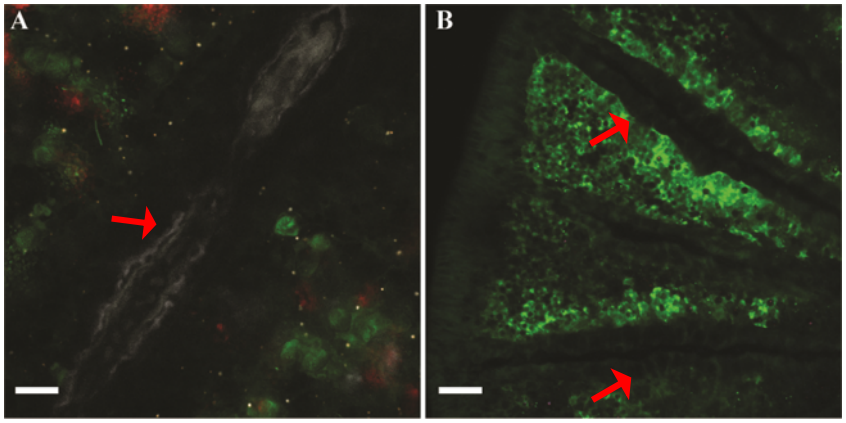

Figure 12- Confocal microscopy of primary polyps of *S. pistillata.* (A) Stained with calcein blue. Calcein fluorescence is displayed in white, green is native auto-fluorescence GFP and red is native auto-fluorescence of the chlorophyll of the dinoflagellate symbionts. This image was taken 14 days after the incubation with calcein and imaging and is used as a positive control for the staining, and the vitality of the coral after the microscopy analysis. The coral continues to grow and precipitate minerals long after the long imaging session. (B) A primary polyp, which has not been incubated with calcein blue. The septa and edge of a primary polyp, have not been stained by calcein blue. This sample is used as a negative control for the staining. Scale bars: **A** 20µm, **B** 50µm. Red arrows - septa.

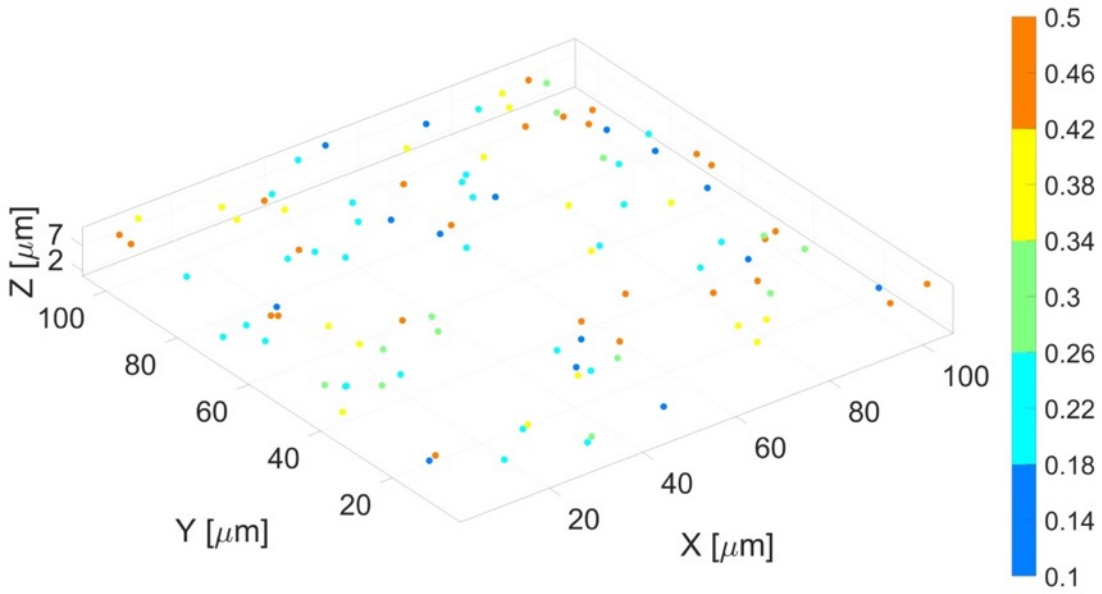

Figure 13- Co-localisation of particles stained with calcein blue and FM 4-64. Co-localisation was quantified as described in[1]. Briefly, a three-dimensional image stack of a live, double-labelled primary polyp was acquired using confocal laser scanning microscopy. Particles were identified in the FM 4-64 channel, and their centroids determined with subpixel accuracy. Particles in the calcein blue channel were then identified, and their centroids determined with subpixel accuracy. If the centroid of an FM 4-64 labelled particle was 0.5 µm or less away from the centroid of a calcein blue-stained particle, they were classified as colocalised, thus showing a particle stained with both FM 4-64 and calcein blue.

In the figure above, coloured dots indicates the colocalisation distances. Blue indicates short distances (i.e. between 0.1 and 0.18 µm), orange indicates longer distances between the membrane marker and the calcein-marked particle (0.42 to 0.5 µm). Colour-coded distances are indicated using the bar on the right. Spatial dimensions (X,Y,Z) are indicated along the axes. The average co-localization distance is 278 ± 118 nm (n=342).

Distances were calculated as described in[3].

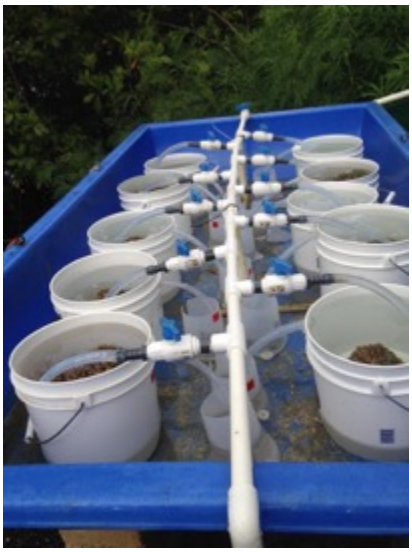

Figure 14- Left: collection buckets set in HIMB during *P. acuta* spawning season in Hawai'i Institute of Marine Biology. Right: Nets set by divers on *S. pistillata* colonies at the Red Sea to collect larvae.

[1] M. Albéric, E.N. Caspi, M. Bennet, W. Ajili, N. Nassif, T. Azaïs, A. Berner, P. Fratzl, E. Zolotoyabko, L. Bertinetti, Y. Politi, Interplay between Calcite, Amorphous Calcium Carbonate, and Intracrystalline Organics in Sea Urchin Skeletal Elements, Crystal Growth & Design 18(4) (2018) 2189-2201.
[2] J.L. Drake, T. Mass, L. Haramaty, E. Zelzion, D. Bhattacharya, P.G. Falkowski, Proteomic analysis of skeletal organic matrix from the stony coral *Stylophora pistillata*, Proc. Natl. Acad. Sci. U. S. A. 110(10) (2013) 3788-3793.
[3] B. Obara, A. Jabeen, N. Fernandez, P.P. Laissue, A novel method for quantified, superresolved, three-dimensional colocalisation of isotropic, fluorescent particles, Histochemistry and Cell Biology 139(3) (2013) 391-402.